Trends in Applied Sciences Research

ISSN 1819-3579

Academic
Journals Inc.

www.academicjournals.com

OPEN ACCESS Trends in Applied Sciences Research

ISSN 1819-3579
DOI: 10.3923/tasr.2020.266.274

Research Article
Integration of Seismic Refraction Tomography (SRT) and Electrical Resistivity Tomography (ERT) to Investigate the Effects of Landslide in Itu L. G. A., Akwa Ibom State, Southern Nigeria

[1]Aka, Mfoniso U., [2]Ibuot, Johnson C., and [3]Agbasi, Okechukwu E.

[1]Department of Physics, University of Uyo, Uyo, Nigeria
[2]Department of Physics, University of Nigeria, Nsukka, Nigeria
[3]Department of Physics, Michael Okpara University of Agriculture, Umudike, Nigeria

Abstract

Background and Objectives: Landslide is a geologic process in which gravity causes rock, soil, artificial fill or a combination of the three to move down a slope and can be activated by the slow weathering of rocks as well as soil erosion. This study aimed to investigate the lithological structures involved in the failure process, determine the landslide material and the influence of groundwater on the landslide occurrence. **Materials and Methods:** Integrated methods of 2D electrical resistivity and seismic refraction tomographies were carried out using resistivity meter and seismography with their accessories spaced at 2 m apart with a total length of 120 m and geo-referenced by differential GPS systems. **Results:** The interpreted results delineate three layer formations: First, second and third layer represent impermeable layer, permeable layer and saturated zones, respectively. Relatively low velocity, elastic and engineering parameters corresponds to the permeable materials in near surface with depth and thickness of about 4.75-11.50 and 4 - 4.75 m with higher porosity. **Conclusion:** These approach reveals that the complexity of the subsoil and sliding processes that affect the slopes movement and rock volume in the area. Hence, the results prove that the study area is liable to landslide and this can affects the environments, motorists and high speed heavy duty trucks movement through the area.

Key words: Seismic Refraction Tomography (SRT), Electrical Resistivity Tomography (ERT), landslide, lithology, higher porosity

Citation: Aka, Mfoniso U., Ibuot, Johnson C. and Agbasi, Okechukwu E., 2020. Integration of Seismic Refraction Tomography (SRT) and Electrical Resistivity Tomography (ERT) to investigate the effects of landslide in Itu L. G. A., Akwa Ibom State, Southern Nigeria. Trends Applied Sci. Res., 15: 266-274.

Corresponding Author: C. Ibuot Johnson, Department of Physics, University of Nigeria, Nsukka, Nigeria

Competing Interest: The authors have declared that no competing interest exists.

Data Availability: All relevant data are within the paper and its supporting information files.

INTRODUCTION

The state of federal roads in the South-south zone of Nigeria has deteriorated to a national disgrace, shame and embarrassment. Calabar-Itu highway road is one of such roads that are a serious nightmare to motorists, commuters and environments with attendant of economic setback (Fig. 1a, b). This highway was constructed over 30 years ago as the only road linking Cross River, Akwa Ibom, Rivers and others South-south and South-east states in Nigeria has become a death trap, particularly during rainy seasons with a serious landslides effects. However, the importance of the Calabar-Itu highway cannot be overemphasized, being a backbone to South-south and South-east states in Nigeria due to its economic significance.

In recent years, the contribution of geophysical methods has became a useful tool to study landslides and to define the boundaries and lithological characteristics[1]. In this study, a landslide occurred after heavy rainfall has been investigated. The maximum amount of rainfall in the landslide area is between the months of March to October every year. Landslide is a collapse of a mass of earth, rock from a mountain or cliff that is one of the natural hazards that claim millions of material and life every year. It occurs in the form of slipping, flowing and falling along a certain surfaces[2]. The detailed characteristics of landslides depict; description of complex phenomena that affect the stability of slopes distribution of fault, fracture zones, water table and sliding surfaces. These anomalies can be investigated by using geophysical investigations, geological mapping, remote-sensing and borehole logging techniques, respectively[3]. However, integrated geophysical technique has been applied to solve a number of problems such as, location of structures in order to better delimit excavations and subsequent stability affected by structural characteristics[4]. However, the dependence of the electrical resistivity parameters such as; rock porosity, water saturation and salinity make the geological interpretation of an inverse model complex and challenging[5]. On the other hand, due to the amount of existing experimental data against the number of parameters required, models and mathematical approximations to solve forward and reserve subsoil problems. Electrical techniques did not give a real coverage information about the subsoil due to its coverage limitation and characterized by a strong uncertainties[6]. Moreover, increase or decrease in fractured zone and the presence of aquifers or rupture surface causes anomalies in electrical resistivity tomographies as explained by Lebourg *et al.*[7]. The current research therefore integrated both seismic refraction and electrical resistivity tomographies to identify slopes instabilities. Because, P and S waves velocity decreases in fractured zones and weathered rock highlighted by lateral changes of velocity models caused by slip surfaces. The analysis of the V_P and V_S wave velocities would delineate elastic, bearing capacity and engineering parameters such as Young's modulus (E), Shear modulus (μ), Poisson ratio (σ), allowable bearing capacity (q_a), concentration index (C_1), material index (V_1), density gradient (D_1) and stress ratio (S_1), respectively[8]. A Seismic Refraction Tomography (SRT) also known as velocity gradient is an imaging geophysical technique that produces across sectional pictures of the subsurface through a non-destructive energy sources such as sledge hammer, weight drop and dynamite charge. It is mostly used for mapping of weathered layer, depth to water table and basement structures for engineering purposes. Moreover, applied in geologic settings where conventional seismic refraction fails such as, areas of compaction, karsts, faults zones and areas with extreme topography or complex near-surface structures[9,10]. Electrical Resistivity Tomography (ERT) technique uses four electrodes for subsurface mapping in order to minimize contact resistivity effects, by injecting an electrical current into the subsurface and measures the potential difference at the surface[11]. It is extensively used in geotechnical, environment and

Fig. 1(a-b): Landslide along Calabar-Itu highway in Akwa Ibom state, Nigeria

engineering to resolve complex geological problems such as; landslides, hidden underground structures and groundwater flows[12]. On the other hand, integrating these independent methods allows constraint to be applied to the inverse problems. In order, to reconstruct subsurface structures, thickness of the mass causing landslides, water content, stratigraphic, lateral lithological variations, bedrock structures and possible detection of cavities. This study aimed to give a more detailed and reliable geometric structures and distribution of physical parameters of the landslides areas.

MATERIALS AND METHODS

Study area: The research study was carried out between the months of June and July to ascertain the shallow and dipping subsurface layer formations in Calabar-Itu. Calabar-Itu highway is situated on the geologic formation of two sedimentary basins namely; Benue trough and Niger Delta basins to the North and South, respectively. The highway alignment traverses the Calabar Flank, which is described by Ekwueme *et al.*[13], as that part of the Southern Nigerian Sedimentary Basin which is bounded by the Oban Massif to the North and the Calabar hinge line delineating the Niger Delta basin in the South as presented in Fig. 2. The sedimentary formation of the area is characterized by Benin Formation, Miocene to recent age, which is also called the Coastal Plain Sands represents the terminal stratigraphic unit in the study area. It comprises mostly of fine to coarse grained, pebbly and moderately sorted sands with local lenses of fine grained, poorly cemented sands and silty clay. The traverse of the highway is made up of the shale units of the Flank namely; the Ekenkpon shale, Nkporo shale and New Netim Marls. The highway is well drained and transects two major rivers namely; Calabar river and Cross river as shown in Fig. 1a and b. The sedimentary succession in the Niger Delta is mostly of tertiary age and is considerably thicker than that of the Benue trough which is dominantly upper cretaceous[14,15]. It is also separated from the Ikpe platform to the west by a NE-SW trending fault. In the east it extends up to the Cameroon Volcanic ridge. Stratigraphically, the Calabar Flank is composed of marine sediments approximately 1000 m thick of Albian to Maastrichtian (Cretaceous) age. The sediments deposited in the Calabar Flank dip gently (normally $<10^0$) mostly to the southwest made up of shales, mudstones, sandstones grits and conglomerates of the Awi Formation[16]. This is followed by the Mid-Albian Mfamosing Limestone, which depicts the first marine incursion of the Calabar Flank[14].

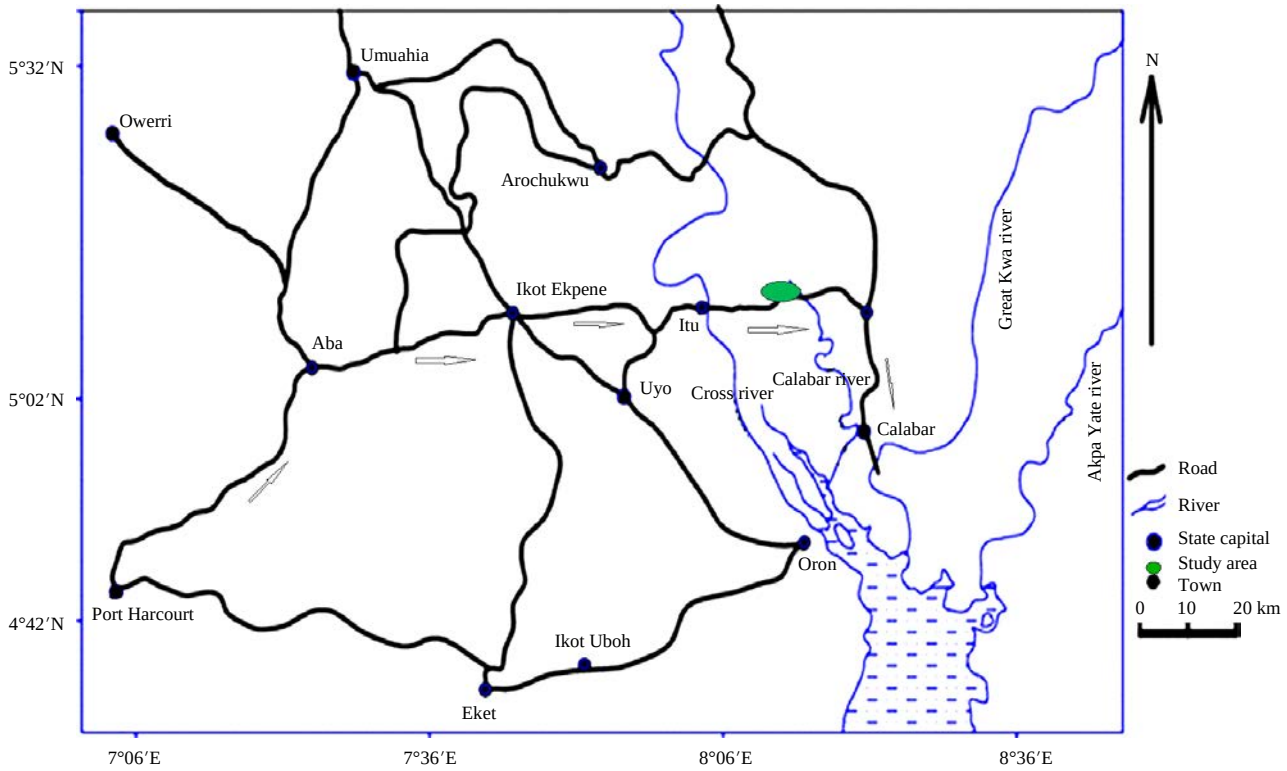

Fig. 2: Location map showing the study area
Source: Adeleye and Fayose[16]

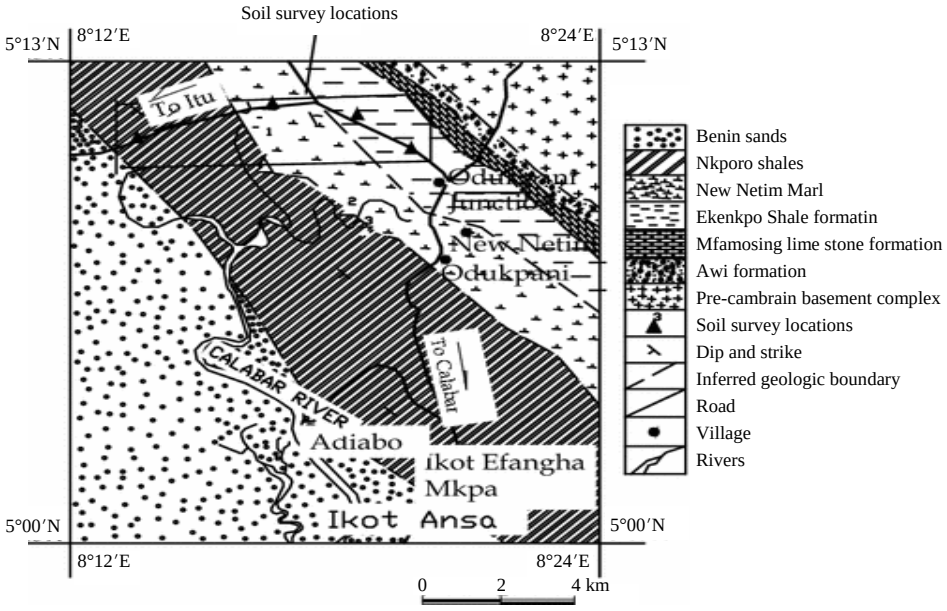

Fig. 3: Geology map of Itu and Calabar flank
Source: Adeleye and Fayose[16]

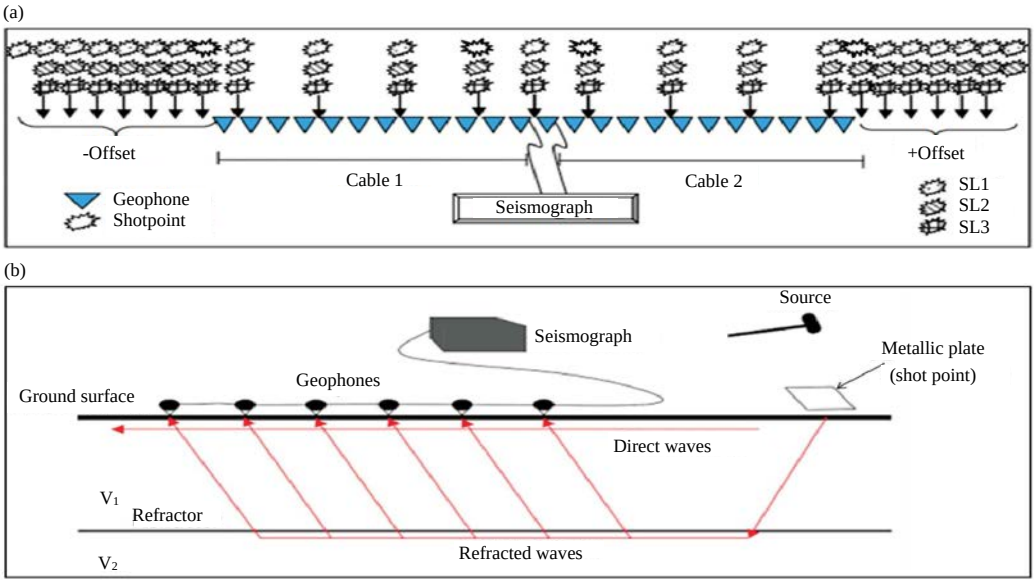

Fig. 4(a-b): (a) Seismic refraction data acquisition lay out and (b) Instrumental setup
Source: Azwin *et al.*[9]

The upland flanks are the Carbonate deposition, calcareous marls are the intervening depression and Ekenkpon shale are the Mfamosing limestone, respectively. The marl is made up of shale fragment, fossil fragments, Calcite and quartz with yellowish colorations[17]. This shale unit is dark grey carbonaceous, friable shale with thin beds of marlstone and gypsum bed as shown in Fig. 3.

Acquisition and processing of geophysical data

Seismic Refraction Tomography (SRT): Acquisition of seismic data required more shot points and receivers at different survey lines or profiles at the earth surface to obtain high quality data. Also, more shot points clusters are requires along offsets distance and geophones for high signal to noise ratio and deeper depth resolutions as shown in Fig. 4a and b.

Seismic refraction tomography was conducted using 24 channels (ES-30000 S) enhancement seismograph. The survey was conducted at 3 profiles with the total length of 120 m, inter-geophone spacing was 2 m with a total of 24 geophones and shot to first geophone offset was 2 m, respectively. A 12 kg sledgehammer was used to generate and transmit seismic waves into the subsurface, 0.5 m diameter aluminum disc was used to receive the sledgehammer strikes with 48 Hz frequency geophone that convert ground motion into electrical analog signal, geophone cables transmit analog electrical impulses from geophones to seismograph and laptop for deposition of data for analysis and processing, respectively. Then, inversion software was used to pick up the first arrival times of P and S waves from the recorded time.

In processing the data, SeisImager package for picking the first arrival time known as PlotRefra and Pickwin software was employed. Three stages were involved in data processing. The first stage involved picking of the first arrival times through visual inspection from collected time record on Pickwin software and stored on the laptop for further analysis. The first arrival times picked were added together and averaged in order to differentiate the first and second layers arrival times. However, the values of arrival times below the averages were taken as first layer while those above the average values were consider as the second layer, respectively and plotted as time (T), distance (X) curves. The T-X curves were plotted based on the profile length, geophone spacing and arrival times. The second stage involved checking and generating of T-X curves through layers and corrected for exact estimation of the P-wave velocity using PlotRefra. The third stage involved modeling of depth-velocity profiles from the observed seismic velocity, which is divided into a number of grid cells or nodes to match the travel times contoured and produced 2D velocity tomography models. Depth-velocity profiles were also modeled and the layered profiles reveal three subsurface layers.

Electrical Resistivity Tomography (ERT): The ERT data were acquired along predetermined traverse along a straight line using Wenner electrode configuration technique to detect the vertical and horizontal variations of subsurface geomaterials. Four sets of multi-cable steels were driven into the ground and a series of take-out of equal electrodes spacing (a) and profiles of length 100 m each. The extended connector sockets from the reference electrode were connected to the switching unit to resistivity meter by multi-core cables. The data was recorded with ABEM SAS 4000 terrameter which measures the resistive property of the subsurface through current injection into the ground.

The measured resistance for different intervals was converted to apparent resistivity using the expression given by Eq. 1:

$$\rho_a = 2\pi aR \quad (1)$$

where, a is the electrodes spacing, R is the field resistance and ρ_a is the apparent resistivity.

The resulting resistivity values were employed to generate the ERT profiles using the RES2DIVN exe software program.

The RES2DINV is a computer program that automatically determines the 2D resistivity model for the data acquired. The program makes inversion by dividing the data into rectangular blocks. The blocks are restrained to the distribution of the data, whereas the depth of the blocks is equal to depth of investigation. The program uses the forward modeling to calculate the apparent resistivity values and a non-linear least-squares optimization technique for inversion routine respectively. The program supported both the finite-difference and finite-element forward modeling techniques. Six steps were involved in the data processing: Noisy and less noisy data with negative values were removed from each profile. Bad data points that have wrong resistivity values due to poor electrode ground contact due to dry soil, shot across the cables to wet ground and relays of electrodes were checked and removed. A trial initial model for the inversion data was made. The RMS error between the observed and calculated apparent resistivity was calculated. Bad data points with large RMS errors were cut-off from original data. The last step was the final inversion modeling. The inversion models give better resolution, smoothen and reduce misfit of failure from the near surface variations.

RESULTS

Three layers of the subsoil were identified: First, second and third both from the seismic refraction tomography and electrical resistivity tomography profiles, respectively. In Fig. 5, the first layer Seismic refraction tomography velocities, V_p and V_s range from 409.80-678.00 and 205.43-392.00 m sec^{-1}, respectively with thickness of 0.00-4.75 m. The Young's modulus, shear modulus and Poisson ratio range from (308.05-1200.24)$\times 10^3$, (70.98-266.72)$\times 10^3$ and 0.25-0.33 N m^{-2}, respectively. The values of allowable bearing capacity range from 86.38-170.08 N m^{-2}. Concentration index, material index, density gradient and stress ratio have values ranging from 4.00-5.00, -0.30-(-0.10), 0.05-0.8 and 0.50-0.30, respectively. In the second layer V_p, V_s and thickness have values ranging from 718.09-915.88, 413.05-704.34 and 5.00-12.25 m, respectively.

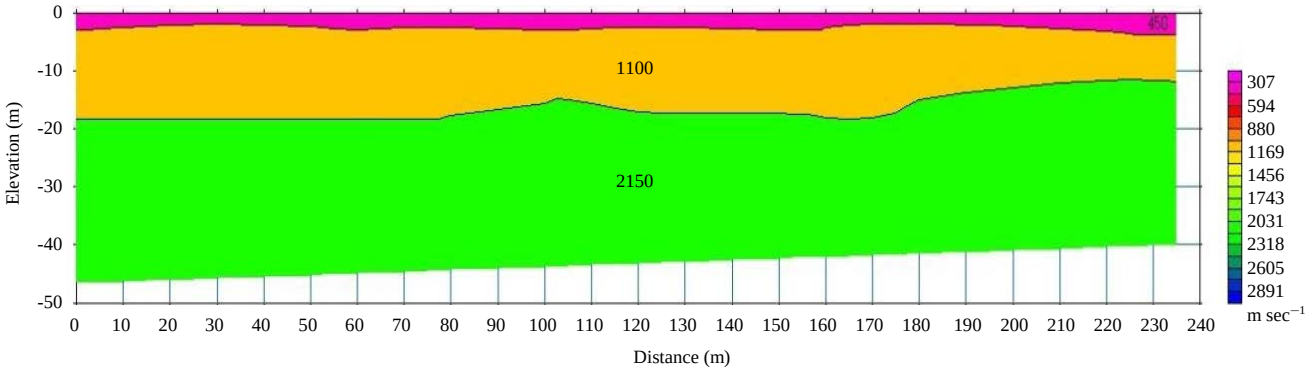

Fig. 5: Inversion seismic refraction tomography velocity depth model profile 1

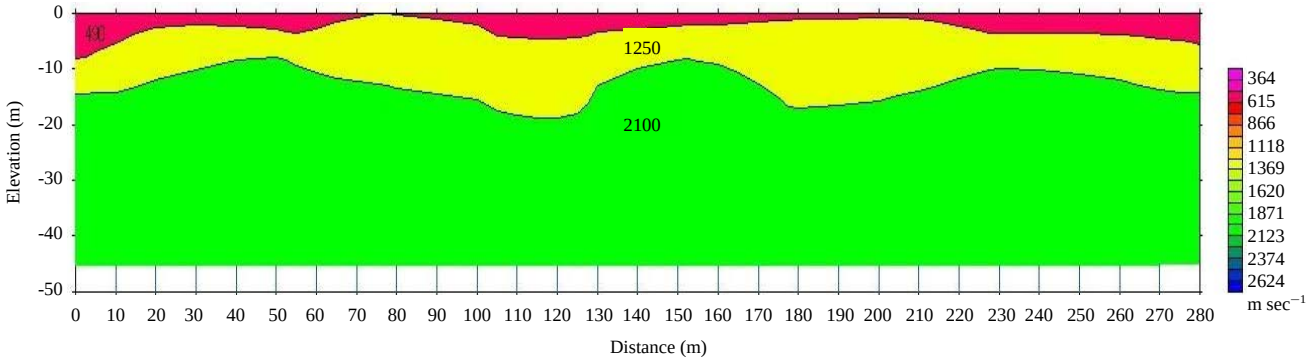

Fig. 6: Inversion seismic refraction tomography velocity depth model profile 2

Young's modulus, Shear modulus and Poisson ratio range from (1300.00-5000.00)×10^3, (300.00-950.00)×10^3 and 0.25-0.22 N m^{-2}, respectively. The values of allowable bearing capacity range from 180.00-350.00 N m^{-2}. Concentration index, material index, density gradient and stress ratio range from 3.30-4.00, 0.10-1.90, 0.13-0.15 and 0.35-0.18, respectively. In the third layer, the values of V_p, V_s and thickness range from 1530.00-2386.00, 1176.50-2094.00 m sec^{-1} and 13.00-24.50 m, respectively. Young's modulus, Shear modulus and Poisson ratio range from (6000.00-13000.00)×10^3, (1403.00-2350)×10^3 and 0.22-0.05 N m^{-2}, respectively. Allowable bearing capacity ranged from 400-550 N m^{-2}. Concentration index, material index, density gradient and stress ratio range from 4.00-5.00, 0.50-2.00, 0.15-0.27 and 0.20-0.05. In Fig. 6, the first layer velocities (V_p and V_s) and thickness have values ranging from 450.00-710.00 and 240.43-410.00 m sec^{-1} and 0.00-4.50, respectively. Second layer has values of V_p and V_s ranging from 800.00-1600.00 and 700.00-1110.00 m sec^{-1} with thickness range of 5.00-12.00 m. In the third layer, the values of V_p and V_s range from 1620.00-2400.00 and 1400.00-2010.00 m sec^{-1}, respectively with thickness ranging from 13.00-22.00 m. In Fig. 7, the first geoelectric layer extends to the depth of about 6 m and resistivity values ranging from 4-20 Ωm. Second geoelectric layer has values of depth and resistivity ranging from 10-13 m and 20-75 Ωm, respectively, while the third geoelectric layer extends to the depth range of about 13.5-19.8 m with resistivity values above 150 Ωm. In Fig. 8, the first geoelectric layer depth extends to a depth of about 6.5 m with resistivity range of 250-400 Ωm, the second geoelectric layer depth ranges from 8-11 m with resistivity values ranging from 550-680 Ωm which covers the entire top soil. The third layer has depth which range from 12.5-19.0 m with a high resistivity values above 900 Ωm. In Fig. 9, the first geoelectric layer depth extends to about 12.5 m with low resistivity values which range from 80-170 Ωm. The second layer depth range from 13-18 m and with resistivity values varying from 300-1080 Ωm. The third layer showed a higher resistivity values which range from 2020-7000 Ωm and thickness above18 m.

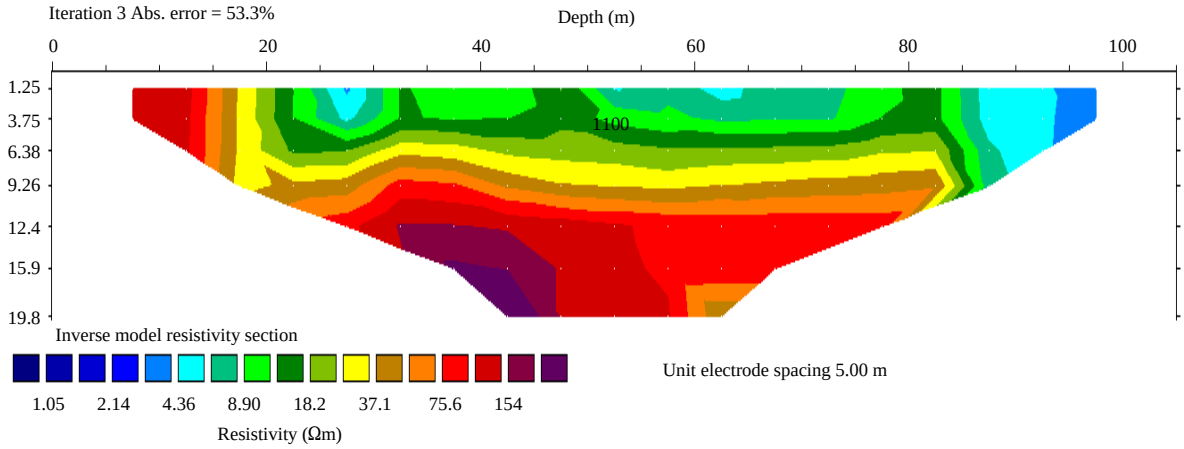

Fig. 7: Inversion electrical resistivity tomography depth model profile 1

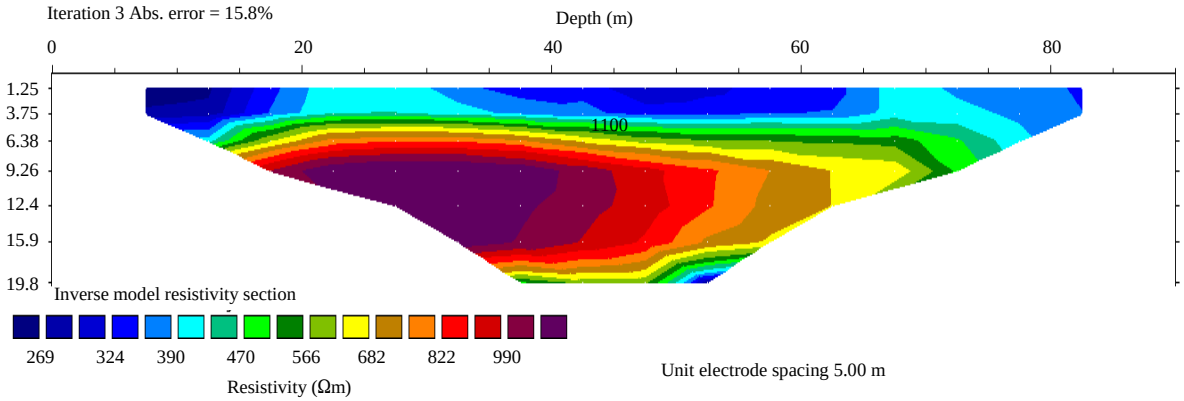

Fig. 8: Inversion electrical resistivity tomography depth model profile 2

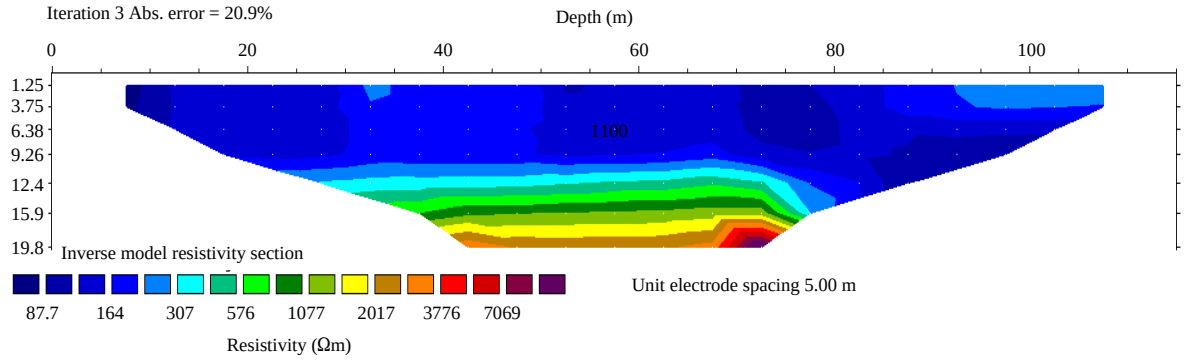

Fig. 9: Inversion electrical resistivity tomography depth model profile 3

In ERT, in profile 1 the first geoelectric layer composed of silty clay (sky blue) and sandy clay (green) colors. The second layer is composed of silty clay loam (green) and clay silt loam (brown) in some areas indicating that the two zones are low resistivity layers which spread across the profile to the depth of about 13 m. Third layer is composed of mostly sand (reddish colour) with high resistivity of about 154 Ωm. In profile 2, the first geoelectric layer is composed of silty loam (blue) and clay loam (sky blue). The second layer is composed of silty loam (green) and clay loam (yellow) with low resistivity which covers the entire topsoil. Third layer is composed of mostly sand (reddish) and light clay (blue colour) with a high

depth and resistivity values. Moreover, in profile 3, the first geoelectric layer is composed of mostly silt (blue colour) with low resistivity values. The second layer is composed of silty loam and sandy clay (green colour) with low resistivity values. The third layer showed a higher depth and resistivity and is composed of sand and gravel (brown colour) along the profile.

DISCUSSION

The major findings of this research study reveal three layers subsoil formations namely: impermeable, permeable and saturated zone as shown in the SRT (Fig. 5, 6) and the ERT profiles (Fig. 7-9), respectively. The importance of this finding includes: In SRT, the first layer subsoil is characterized by saturated water formation, relative high porosity and permeability. Also, the allowable bearing capacity encountered is associated with zones that are highly drained with water. The engineering parameters depict high stress ratio and low concentration index indicating that the zone is completely filled with water. The second layer is characterized by porous permeable formation, rock/unconsolidated sediments and moderately/unsaturated water formation. The third layer characterized by solid impermeable layer that does not allow water to penetrate the surface. This indicated good materials/soil stability as most eligible layer for engineering purposes. It could be inferred from this study that landslide could be triggered by heavy rainfall, soil composition, topography of the area and in increase in soil weight[1,2,7]. The disparity encountered between the profiles in the variation of resistivity is most probably due to the changes in soil composition in different directions[7,18-20]. The variations observed in various layers of the subsurface could also be attributed to compaction and cementation which increases with depth[19]. These similarities between SRT and ERT findings proved the method vital tools to geophysicists and engineers for detecting of landslide effects.

CONCLUSION

This study delineates the subsurface layer formations comprising of impermeable, permeable and saturated zones. The refinements in imaging version techniques, through these new integrated methods have greatly improved the data quality for resolving complex subsurface features. These approaches obtained subsurface models that agreed with the calculated field models for the velocities and resistivities of earth's subsurface features. The findings will provide information that will be useful to engineers in order to construct roads that will withstand the load of heavy duty vehicles/trucks passing through the area, minimizing the destruction of properties and fast track economic development in the area. Hence, integrated inversion techniques is accurate, efficient, faster and gives higher resolution inversion models for investigating subsurface cavities such as landslides.

SIGNIFICANCE STATEMENT

This study discovers the third layer subsoil formation characterized by competent impermeable materials to be beneficial for geotechnical engineering purposes. This study will help other researchers to uncover the critical areas of landslide effect, boundaries and lithological characteristics by applying the integrated methods. This study has thrown more light to the understanding of landslide, effects, control and the importance of integrating SRT and ERT to study landslide.

REFERENCES

1. Cosentino, P., R. Martorana, M. Perniciaro and L.M. Terranova, 2003. Geophysical study of an landslide in Northern Sicily. Near Surface Geophys., 1: 77-84.
2. Yamao, M., R.C. Sidle, T. Gomi and F. Imaizumi, 2016. Characteristics of landslides in unwelded pyroclastic flow deposits, Southern Kyushu, Japan. Nat. Hazards Earth Syst. Sci., 16: 617-627.
3. Chianese, D., V. Lapenna, S. Di Salvia, A. Perrone and E. Rizzo, 2010. Joint geophysical measurements to investigate the rossano of vaglio archaeological site (Basilicata region, southern Italy). J. Archaeol. Sci., 37: 2237-2244.
4. Wegmann, K.W., D.R. Bohnenstiehl, J.D. Bowman, J.A. Homburg, J.D. Windingstad and D. Beery, 2012. Assessing coastal landscape change for archaeological purposes: Integrating shallow geophysics, historical archives and geomorphology at Port Angeles, Washington, USA. Archaeol. Prospection, 19: 229-252.
5. Jongmans, D. and S. Garambois, 2007. Geophysical investigation of landslides: A review. Bull. Société Géologique France, 178: 101-112.
6. Pazdirek, O. and V. Blaha, 1996. Examples of resistivity imaging using ME-100 resistivity field acquisition system. Proceedings of the EAGE 58th Conference and Technical Exhibition Extended, June 1996, European Association of Geoscientists & Engineers.
7. Lebourg, T., S. Binet, E. Tric, H. Jomard and S. El Bedoui, 2005. Geophysical survey to estimate the 3D sliding surface and the 4D evolution of the water pressure on part of a deep seated landslide. Terra Nova, 17: 399-406.
8. Aka, M.U., F.N. Okeke, J.C. Ibuot and D.N. Obiora, 2018. Geotechnical investigation of near-surface structures using seismic refraction techniques in parts of Akwa Ibom State, Southern Nigeria. Mod. Earth Syst. Environ., 4: 451-459.

9. Azwin, I.N., R. Saad and M. Nordiana, 2013. Applying the seismic refraction tomography for site characterization. APCBEE Procedia, 5: 227-231.
10. Gregory, S.B., 2002. Near-surface seismic refraction tomography tutorial. UB Geophys. Rep.
11. Daily, W., A. Ramirez, A. Binley, D. LaBrecque and D.L. Alumbaugh *et al*., 2005. Electrical Resistance Tomography-Theory and Practice. In: Near Surface Geophysics (Investigations in Geophysics Series 13), Butler, D.K. (Ed.)., Society of Exploration Geophysicists, USA., ISBN: 978-1560801306, pp: 525-550.
12. Dahlin, T. and B. Zhou, 2004. A numerical comparison of 2D resistivity imaging with 10 electrode arrays. Geophys. Prospect., 52: 379-398.
13. Ekwueme, B.N., E.E. Nyong and S.W. Petters, 1995. Geological Excursion Guidebook to Oban Massif, Calabar Flank and Mamfe Embayment, Southeastern Nigeria. Dec. Ford, Calabar.
14. Petters, S.W., 1980. Biostratigraphy of upper cretaceous foraminifers of the benue trough, Nigeria. J. Foraminifera Res., 10: 191-204.
15. Petters, S.W. and C.M. Ekweozor, 1982. Petroleum geology of benue trough and Southeastern Chad Basin, Nigeria. AAPG Bull., 66: 1141-1149.
16. Adeleye, D.R. and E.A. Fayose, 1978. Stratigraphy of the type section of Awi Formation, Odukpani Area, South-Eastern Nigeria. Niger. J. Min. Geol., 15: 33-37.
17. Reyment, R.A., 1965. Aspects of the Geology of Nigeria. Ibadan University Press, Ibadan, Nigeria.
18. Ilori, A.O., 2016. Occurrence of shale soils along the Calabar-Itu highway, Southeastern Nigeria and their implication for the subgrade construction. SpringerPlus, Vol. 5. 10.1186/s40064-016-1822-4
19. George, N.J., J.B. Emah and U.N. Ekong, 2015. Geohydrodynamic properties of hydrogeological units in parts of Niger Delta, Southern Nigeria. J. Afr. Earth Sci., 105: 55-63.
20. Agada, I., J.C. Ibuot, M. Ekpa and D.N. Obiora, 2017. Investigation of subsurface for construction purposes in Makurdi, Benue State, Nigeria, using electrical resistivity method. J. Geol. Min. Res., 9: 9-17.